Jurnal ELEMENTER
(Elektro dan Mesin Terapan)
Vol. 11, No. 01, Mei 2026
DOI: 10.35143/ elementer.v11i1
P-ISSN: 2443-4167
E-ISSN: 2460-5263

Numerical Study of the Effect of Grid Number and Viscous Model on Fin and Tube Heat Exchanger Performance

Muhamad Safi'i[1*], Nazaruddin Sinaga[2], Eflita Yohana[3], Yafid Effendi[4], Akhmad Irfan[5], Suheri Suheri[6], Rouf Muhammad[7], Agung Nugroho[8], Candra Wahyu Sportyawan[9]

[1*] Department of Mechanical Engineering, Faculty of Engineering and Informatics, Persatuan Guru Republik Indonesia Semarang University, 50232, Indonesia.
[2,3] Department of Mechanical Engineering, Faculty of Engineering, Diponegoro University, 50275, Indonesia.
[4] Department of Mechanical Engineering, Faculty of Engineering, Muhammadiyah Tangerang University, 15118, Indonesia.
[5] Department of Mechanical Engineering, Faculty of Engineering and Computer Science, Sains Al Qur'an, Central Java, Wonosobo University, 56351, Indonesia.
[6] Department of Mechanical Engineering, Faculty of Sains and Technology, Samudra University, Langsa, Aceh, 24416, Indonesia.
[7] Department of Mechanical Engineering, Faculty of Engineering, Jakarta Politecnic of State PSDKU Demak, 59516, Indonesia.
[8] Department of Mechanical Engineering, Faculty of Engineering, Wahid Hasyim University, 50323, Indonesia.
[8] Department of Mechanical Engineering, Faculty of Engineering, Pandanaran University, 50268, Indonesia.

Corresponding Author: muhamadsafii@upgris.ac.id.

Article History
Submitted: 14 March 2026
Revised: 16 May 2026
Accepted: 28 May 2026
Published: 31 May 2026
Available online: 31 May 2026

Abstract
Fin and tube heat exchanger (FTHE) has attracted attention among technicians and researchers due to its performance. This research was conducted to determine the effect of variations in the number of grids and viscous models on FTHE on its thermal performance using the Fluent application in the Computational Fluid Dynamics computer program which was varied against the number of grids and viscous models at various fluid flow speeds with a constant heat flux of 100 W. This optimization study was conducted to find the best settings in numerical studies. The best results of this research were obtained that the variation of the longitudinal pitch ratio of 14.5 mm with a heat transfer coefficient value of 97.24 W/m²K, while the transverse pitch ratio of 11.7 mm with a heat transfer coefficient value of 107.82 W/m²K. The best results of this study were obtained at a variation of the number of grids of 358456 in the variation of the viscous k-ω Standard model with an average FTHE temperature value of 21.35℃ and a maximum heat transfer coefficient value of 101.74 W/m²K. These results confirm that the variation of the number of grids of 358456 in the variation of the viscous k-ω Standard model allows that the numerical study model can be recommended and used for practical applications in machine devices and can be applied directly in the field such as petrochemical processing devices, HVAC&R, and other devices.

***Kata kunci**: Fin and Tube Heat Exchanger (FTHE), Longitudinal Pitch, Transversal Pitch, Performance.*

1. Introduction

Fin and tube heat exchangers (FTHE) have attracted attention among engineers and researchers due to their performance [1]. Generally, fin and tube heat exchangers (FTHE) are applied in refrigeration, petrochemical, and HVAC&R systems, due to their easy fabrication, simple construction, low cost, and ease of maintenance [2, 3, 4]. Improving the thermal and hydraulic performance of FTHEs is a major concern due to increased energy efficiency, the ability to control pressure drops, and the ability to improve effective cooling performance [4, 5]. The installation of tubes in FTHEs has been proven to effectively improve thermal and hydraulic performance with high efficiency [6]. However, the accumulation of dirt due to the close proximity of the tubes causes blocking in the FTHE, which in turn can cause blocking, thus reducing its thermal performance [7]. Therefore, a series of maintenance and repairs is required [8]. However, modifications in various ways, such as embossing, mounting, or punching, are carried out to improve thermal and hydraulic performance [9]. The type H with an inline and staggered tube arrangement is characterized to improve thermal and hydraulic performance, resulting in an increase in Nusselt number by 7% in the inline arrangement and 5% and staggered arrangement [10]. The duct length ratio was developed with dimension variation of 44.3 m to 48.7 m in the FTHE air-to-ground heat exchanger; the result is that the duct length ratio of 44.3 m to 48.7 m can increase efficiency and thermal performance by 70% [11].

Axial and radial FTHE with circle tube geometry were studied considering its pitch ratio of 10% mm. As a result, a decrease in the tube surface temperature value of 2ºC was obtained, so that the effectiveness could be increased by 10% [12]. The shape of wedge-shaped fins with a shape angle ratio of 0º and 60º was studied. The best results were found in wedge-shaped fins with a shape angle ratio of 60º, with a substantial temperature reduction value of 80% [13]. The shape of bow-shaped vortex generators in FTHE was studied using numerical methods by considering variations in the thickness of the vortex generator of 1 mm, 3 mm, and 5 mm, as well as a viscous model during the numerical study. It was proven that the Nusselt number of 1 can be increased by 8% [14]. The wavy fin spacing of 1.3 mm and 2.3 mm, arranged in line and staggered, was studied regarding the characteristics of fluid flow and heat transfer at various Reynolds numbers. The geometric shapes of the tube in the form of a circle, oval, and airfoil shape with wavy fin spacing ratio were considered in this research. The best results were obtained in FTHE with a circle-shaped tube with a fin spacing ratio of 2.3 mm arranged inline with an increase in Nusselt number of 30% to 40% [15].

FTHE with trapezoidal slit fin geometry was characterized by numerical studies. Variations in slit fin heights of 0.98 mm, 1.225 mm, 1.47 mm, and 1.715 mm were proposed in this study. Optimal results were obtained in FTHE with 1.47 mm trapezoidal slit fins with a heat transfer coefficient of 130 W.m².K and the highest Nusselt number of 70 [16]. The use of PCM materials has attracted attention for cooling fluid applications in FTHE. It is expected that PCM materials can improve the heat transfer and efficiency of FTHE [17]. PCM types A27 and RT35 were applied to FTHE to cool the device. It is known that variations of twisted and straight fins were proposed and considered in FTHE by experimental and numerical methods. The best results were obtained when the PCM RT35 material was able to improve the heat transfer by 14% for twisted and 40% for straight fins. These results confirm that the PCM RT35 material is an ideal PCM material for application in FTHE [18].

Air flow velocities of 7 m/s, 8.56 m/s, 9 m/s, and 10.56 m/s were proposed in experimental and numerical studies on FTHE. The goal was to improve the heat transfer performance. The results of experimental and numerical studies found that the tube surface temperature could be reduced by up to 10ºC, and the Nusselt number value was obtained up to 7% [10, 19]. FTHE with helically coiled copper tube geometry was studied regarding its heat transfer performance by applying organic PCM material as a cooling fluid. Variations in pump rpm of 200 rpm and 400 rpm were proposed. The results showed that the tube surface temperature could be reduced by 2º for 200 rpm and 3.5ºC for 400 rpm. These results were also able to increase the heat transfer coefficient value by around 39.6% [20].

A computational domain with dimensions of 72.2 x 25.4 x 1.96 mm was created considering grid numbers of 1000000, 2000000, and 3000000 as optimization material for the thermal performance of FTHE. In the setup of the numerical study, the k-ω BSL model was applied. As a result, a 20% increase in the Nusselt number made it the optimal setting in the numerical study being studied [3]. Variations in grid numbers of 1000000, 1500000, 2000000, 2500000, and 3000000 in the numerical study of finned shell and coil heat exchangers were developed to determine their performance. The viscous k-ω Standard model was applied in this numerical study. As a result, the variation in grid numbers of 3000000 had the best results in this study. It was found that the maximum heat transfer coefficient value was 780 W.m²K [21]. Grids of 1350000, 1670000, and 2010000 were developed to characterize the thermal and hydraulic performance of finned-curved tubes compact heat exchanger. The viscous k-ω Standard, k-ω SST, and k-ω BSL models were also considered in this research. The results showed that the number of grids of 2010000 with the viscous k-ω Standard model had good thermal and hydraulic performance. It was found that the Nusselt number could be increased by 8%, namely 12.5, so that the PEC value increased and the highest value was obtained with a value of 1.5 [22].

Many studies have been conducted on FTHE, both experimental and numerical, to understand the increase in heat transfer with various geometry variations, such as circular, oval, egg-shaped tubes, arrays of tubes in rows, spread arrays, geometric ratios, fluid flow velocities, heat fluxes, and others. However, until now, there has been no research using numerical methods with Computational Fluid Dynamics (CFD) software on FTHE with elliptical tube shapes. Variations in the number of grids and the viscous model k-ω are proposed in this study by considering variations in fluid flow velocities of 0.5, 1, 1.5, 2, 2.5, 3, and 3.5 m/s with a constant heat flux of 100 W to determine the optimum number of grids, a suitable viscous model, and the optimum thermal and hydraulic performance. For this reason, a numerical study on FTHE was conducted. The results of this study are expected to obtain the optimum number of grids and the most suitable viscous model for numerical studies in terms of thermal and hydraulic performance, where the results of this research are expected to be used as recommendations and applied for practical applications in the field.

2. Methods

2.1. Physical Model

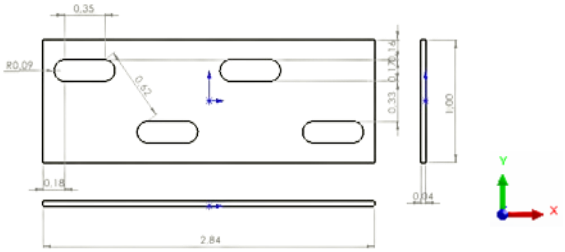

Figure 1. FTHE Geometry.

Figure 1 depicts the FTHE structure created using SolidWorks software, referring to previous research [3], with the dimensions of the FTHE test section being length x width x height 72.2 x 25.4 x 1.96 mm. Furthermore, we introduce innovations in this research in the form of variations in the number of grids of 157653, 257892, and 358456 with variations in fluid flow velocity between 0.5 m/s, 1 m/s, 1.5 m/s, 2 m/s, 2.5 m/s, 3 m/s, and 3.5 m/s, as well as a fixed heat flux of 100 W. The viscous k-ω Standard, k-ω SST, and k-ω BSL models are also considered in this research.

2.2. Materials

Aluminum alloy 6061 was selected for the FTHE module. Its thermal conductivity was estimated at k = 168 (W/m.K). The surrounding air that functions as a coolant with a temperature of 25ºC in this study has material characteristics with a density of ρ = 1.2096 kg/m³, a specific heat capacity of Cp = 1005 J/kg.K, viscosity of μ = 1,915×10^{-5} kg/ms, a thermal conductivity of k = 0.0261 W/m.K, and a molecular weight of m = 28.966 kg/kmol. These parameters were entered based on the Ansys database found in the settings menu of the Fluent application in the Computational Fluid Dynamics (CFD) program.

2.3. Numerical Study

Figure 2 shows the numerical analysis boundary conditions for single-phase flow through an FTHE in a steady state. The computational domain was created using the modeler design menu in the Fluent application included in the Computational Fluid Dynamics

(CFD) program, with dimensions of 28.8 x 25.4 x 1.96 mm for the water inlet area and 216.6 x 25.4 x 1.96 mm for the water outlet area. The computational domain is divided into three zones: the upstream region, the test section, and the downstream region. The upstream region aims to ensure that the air flow entering the test section is even. After that, the air enters the test section, which consists of two rows of elliptical pipes in a longitudinal and transverse arrangement. When the air passes through the test section, it enters the downstream region, which functions to prevent the flow back into the test section.

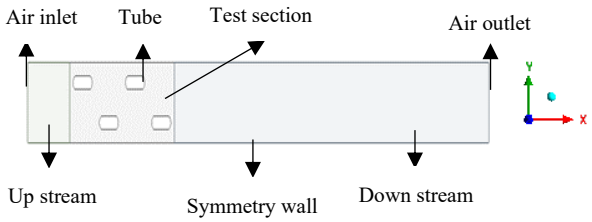

Figure 2. Computational Domain of FTHE.

2.4. Meshing

The computational mesh applied in the numerical analysis is shown in Figure 3. The control volume method is used to discretize the equations governing the first-order upwind scheme to provide more precise calculation results generated in the mesh setup menu. The computational area is created with a fully structured tetrahedral mesh and has a high resolution near the wall to capture the effects of the bat layer.

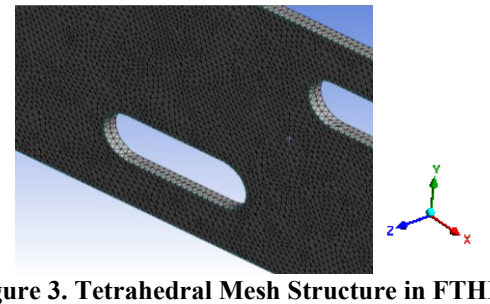

Figure 3. Tetrahedral Mesh Structure in FTHE.

The continuity, momentum, and energy equations for numerical studies on OFHS with the forced convection method are shown by:

Continuity equation:

$$\frac{\partial u}{\partial x}+\frac{\partial v}{\partial y}+\frac{\partial w}{\partial z}=0 \qquad (1)$$

$$\rho\left(u\frac{\partial u}{\partial x}+\frac{\partial u}{\partial y}+w\frac{\partial u}{\partial z}\right)=\frac{-\partial P}{\partial x}+\mu\left(\frac{\partial^2 u}{\partial x^2}+\frac{\partial^2 u}{\partial y^2}+\frac{\partial^2 u}{\partial z^2}\right) \qquad (2)$$

$$\rho\left(u\frac{\partial v}{\partial x}+v\frac{\partial v}{\partial y}+\frac{\partial v}{\partial z}\right)=\frac{-\partial P}{\partial x}+\mu\left(\frac{\partial^2 v}{\partial x^2}+\frac{\partial^2 v}{\partial y^2}+\frac{\partial^2 v}{\partial z^2}\right) \qquad (3)$$

Momentum equation:

$$\rho\left(u\frac{\partial w}{\partial x}+v\frac{\partial w}{\partial y}+\frac{\partial w}{\partial z}\right)=\frac{-\partial P}{\partial x}+\mu\left(\frac{\partial^2 w}{\partial x^2}+\frac{\partial^2 w}{\partial y^2}+\frac{\partial^2 w}{\partial z^2}\right) \qquad (4)$$

Persamaan energi:

$$\rho Cp\left(u\frac{\partial T}{\partial x}+v\frac{\partial T}{\partial y}+\frac{\partial T}{\partial z}\right)=k\left(\frac{\partial^2 T}{\partial x^2}+\frac{\partial^2 T}{\partial y^2}+\frac{\partial^2 T}{\partial z^2}\right) \qquad (5)$$

2.5. Grid Independent Test

A grid test was conducted to determine the optimal number of grids in analyzing the impact of longitudinal and transverse pitch variations on the thermal performance of FTHE. In this process, the mesh size with element size variations of 157653, 257892, and 358456 was known. The grid test results are shown in Figure 4. There is a relationship between the grid number and the Colburn Factor, J value. From the calculation in the numerical study on the grid test, the relative error between grids 157653 and 257892 was obtained at ±3% with a Colburn Factor, J value of 0.0061; while for grids 257892 and 358456, the error was ±1% with a Colburn Factor, J value of 0.0065.

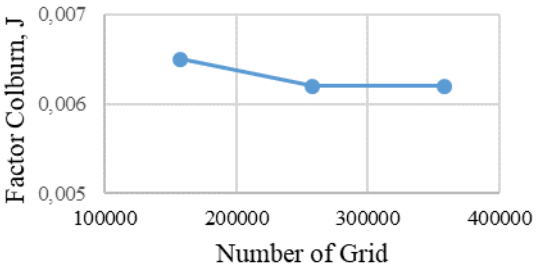

Figure 4. Grid Test Graph.

The mesh count of 358456 was chosen because, in independent grid testing, when the mesh count was increased from 257892 to 358456, a very small difference was obtained in the Colburn Factor, J value of 0.00012. If the mesh count was increased again from 358456 to 400000, it is likely that the Colburn Factor, J value would only increase by about 5% from the value of 0.00012, and there would be no significant difference. Therefore, the mesh count of 358456 is considered the most ideal number.

2.6. Validation

Validation was conducted using numerical methods against experiments found in the literature [3] on FTHE specimens through forced convection. In this study, the parameters to be sought are the tube surface temperature to calculate the heat transfer coefficient, Nusselt number, and Colburn Factor, J, on the newly proposed FTHE. This validation process involves a comparison between variations in the number of grids and the Colburn Factor, J value of the FTHE. The results of the validation can be seen in Figure 4, which shows the relationship between Reynolds number and Colburn Factor, J. From the graph, the experimental results listed in the literature [3] show that the Colburn Factor, J value is 0.0092, while the Colburn Factor, J value obtained in the current study is 0.0094 for a Reynolds number of 1300. When comparing the numerical results with the forced convection method on FTHE against the experimental data from the literature, it was found that the largest relative error (or uncertainty of the numerical results compared to the experiments in the literature) was 0.9%. The validation results showed the largest relative error with a value of 1.1% and a Colburn Factor, J of 0.0078 at a Reynolds number of 1650. These findings indicate a good agreement between the experimental results from the literature [3] and the numerical study currently in the validation process.

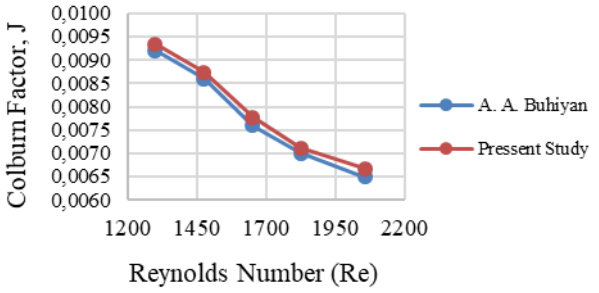

Figure 5. Relationship between Reynolds Number and Colburn Factor, J.

Validation was conducted using a numerical approach and comparing with experiments conducted in the literature [3] on FTHE specimens through the forced convection method. The focus of this study was to obtain the pipe surface temperature parameters to determine the heat transfer coefficient, Nusselt number, Colburn Factor, and J values in the newly proposed FTHE. The validation process was conducted by comparing the variation of the number of grids with the Colburn Factor, J value of the FTHE. The results of the validation process are shown in Figure 5, which shows the relationship between the Reynolds number and the Colburn Factor, J value. From the graph, it can be seen that the experimental results from the literature [3] produced a Colburn Factor, J value of 0.0092, while the value being studied is 0.0094 at a Reynolds number of 1300. When comparing the numerical results with the forced convection method on FTHE with experiments from the literature based on the Colburn Factor, J value, the largest relative error (uncertainty of the numerical results compared to the experiment) was found to be 0.9%. Validation shows that the largest relative error is 1.1% with a Colburn Factor, J of 0.0078 at a Reynolds number of 1650. This finding shows good consistency between the experimental results from the literature [3] and the numerical study being validated.

2.7. Numerical Data Reduction

The operating conditions of the FTHE during the numerical study were based on the experimental study of [3]. In this research, it was assumed that the specific heat is defined as the

amount of heat required to raise the temperature of a sample of a substance by one degree, thus obtaining the following equation:

$$C_p = \frac{Q}{m\Delta T} \quad (6)$$

Where P_{in} is the inlet pressure, and the heat flux is calculated using the equation:

$$Q = \dot{m}(T - T_{in}) = \rho.U.A_c.c(T - T_{in}) \quad (7)$$

Logarithmic Mean Temperature Difference is defined by the equation:

$$LMTD = \frac{((T_{wall} - T) - (T_{wall} - T_{in}))}{ln\left(\frac{(T_{wall} - T)}{(T_{wall} - T_{in})}\right)} \quad (8)$$

The local heat transfer coefficient is considered based on the heat flux input and the LMTD calculation results on the FTHE, so that the heat transfer coefficient can be calculated using the equation:

$$h = \frac{Q}{A_a \times LMTD} \quad (9)$$

The local heat transfer coefficient values can be correlated to calculate the Nusselt number value, so that:

$$Nu = \frac{h.H}{k} \quad (10)$$

The friction factor and Colburn Factor, J, are calculated using the equation:

$$f = \frac{(P_{in} - P)}{\frac{1}{2}.\rho u_{in}^2}.\frac{H}{4L} \quad (11)$$

$$j = \frac{Nu}{Re.Pr^{1/3}} \quad (12)$$

Heat transfer equation per unit fan:

$$Q/P_f = \frac{Q}{\Delta p \times \dot{m}/(\rho \times \eta_f)} \quad (13)$$

3. Result and Discussion

3.1. Effect of Grid Number on FTHE Performance

Essentially, the examination of the impact of varying grid numbers during the numerical study on FTHE performance begins with airflow entering through the air inlet in the upstream domain with varying airflow velocities: 0.5 m/s, 1 m/s, 1.5 m/s, 2 m/s, 2.5 m/s, 3 m/s, and 3.5 m/s at a temperature of 25ºC and a constant flux of 100 W. This air then serves to cool the tube in the test section and gradually flows out into the downstream domain channel.

Variations in grid numbers of 157653, 257892, and 358456 are proposed and characterized against various viscous models in the numerical study being studied to analyze the thermal performance of the FTHE. Only the best results are presented in this research. Variations in grid numbers play a significant role in the thermal performance of the FTHE. A higher grid number improves the accuracy of the calculation of the convective heat transfer coefficient and temperature distribution. A denser mesh, especially near the boundary layer, is essential to capture sharp temperature gradients, which are crucial for predicting the effectiveness of the FTHE. Figure 6 illustrates the FTHE temperature contours with respect to the variation of the grid number with respect to the variation of the Standard viscous k-ω model.

It can be seen that with a variation in air flow velocity of 3.5 m/s with a constant heat flux at a grid number of 157653, there are obstacles or structures in the channel that cause flow disturbances, resulting in a thin thermal boundary layer. It is possible that the grid number of 157653 has a meeting of low-temperature air near the tube wall caused by centrifugal force, which has less significant effect on increasing the heat transfer rate. At a grid number variation of 257892, it can be seen that the thermal boundary layer tends to develop; this is due to the effect of mesh density, which allows the capture of the thermal boundary layer to be almost accurate. At a grid number variation of 358456, it is proven to have high thermal boundary layer characteristics. The cause is the high mesh cell number that

allows numerical studies on FTHE to show maximum results due to mesh density.

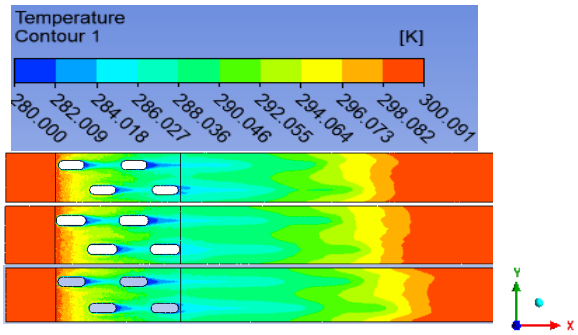

Figure 6. FTHE Temperature Contour with Variations in the Number of Grids of 157653, 257892, and 358456 and Variations in Flow Velocity of 3.5 m/s.

So that the thermal performance effect is good. With too many grids (too fine), the numerical study conducted will drastically increase the computation time and memory requirements, and provide a significant increase in accuracy after reaching the optimal point. Finer grids are needed in FTHE areas with high temperature gradients or velocities, such as around the tube or near the tube wall, to more accurately model the boundary layer, which is characterized by a significant decrease in the tube surface temperature. The large number of grids in the FTHE numerical study causes the temperature distribution contour to experience resistance, which leads to the formation of temperature swirl flow. This swirl flow may be considered as randomizing the temperature contour. However, when the numerical process takes place, this phenomenon actually increases the thermal boundary layer around the tube, resulting in more even tube cooling.

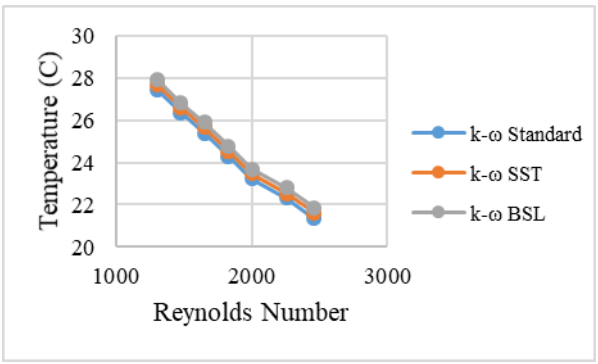

Figure 7. Graph of Temperature Values and Reynolds Numbers on Grid Variations 358456.

Figure 7 shows that overall, the graph shows a decreasing temperature trend with increasing Reynolds number. At low Reynolds numbers (around 1300), the average surface temperature of the FTHE is highest (around 28ºC), and at high Reynolds numbers (around 2500), the average surface temperature of the FTHE drops to its lowest point (around 21ºC-22ºC). An increase in Reynolds number typically indicates an increase in flow velocity or a transition from laminar to turbulent flow. Faster or more turbulent flow increases the convective heat transfer coefficient (h). Consequently, heat loss from the system to the fluid becomes more effective, resulting in a decrease in the temperature of the object or fluid being measured.

This shows that for the Reynolds number range of 1300 to 2500, the simulation results are quite consistent and stable regardless of the variations in the viscous model used. Small differences between the three models may be due to how each model handles calculations near walls (wall functions) or in the boundary layer. These results confirm that increasing the flow rate (represented by the Reynolds Number) directly increases the cooling efficiency in the simulated system, with variations in the turbulence model giving very similar results to each other.

Figure 8 explains that as the Reynolds Number increases (which reflects an increase in fluid flow velocity), the intensity of turbulence in the fluid also increases. The impact of higher turbulence increases fluid particle mixing and thins the thermal boundary layer. As a result, the resistance to heat transfer is reduced, so that the heat transfer coefficient value increases significantly. k-ω Standard (Blue): Shows a slightly higher coefficient value than the other two models in almost the entire range. This model is very good for near-wall flow (near-wall treatment). k-ω SST (Shear Stress Transport) (Orange): Is a development of the Standard model. This model is usually more accurate in predicting the occurrence of flow separation because it combines the advantages of the near-wall model and the free-stream model. k-ω BSL (Baseline) (Gray): Shows results very similar to the SST model. This model serves as a link between the k-ω Standard model and the k-ε model. All three models show consistent and very close trends. This indicates that for this flow case, the selection of the k-ω variant does not produce drastic differences in the data, so that the

simulation results can be said to be quite stable and reliable.

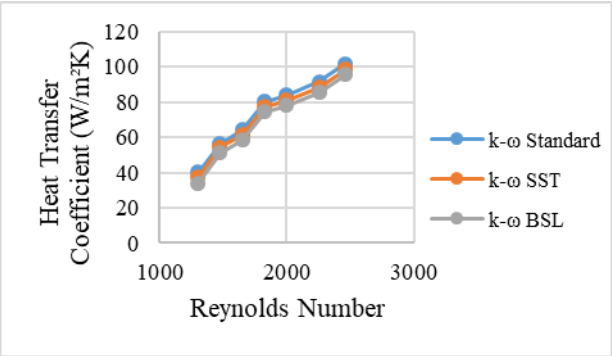

Figure 8. Graph of Heat Transfer Coefficient and Reynolds Number Values on Grid Variations 358456.

At Reynolds number 1300, the heat transfer coefficient value is in the range of 35-40 W/m²K, and at Reynolds number 2500, the heat transfer coefficient value increases sharply to reach the range of 95-100 W/m²K. However, strangely, there is a fairly steep increase at the beginning at Reynolds number 1300-1800 with a heat transfer coefficient value of around 80 W/m²K, which may indicate a transition from laminar to turbulent flow or a change in the thermal characteristics of the geometry. Overall, this graph proves that increasing the flow velocity (Reynolds Number) effectively increases the heat transfer efficiency. The Standard k-ω model tends to provide slightly more optimistic (higher) estimates than the SST k-ω and BSL k-ω models in predicting the thermal performance of this system.

3.2. Effect of Viscous Model on FTHE Performance

With the varying grid size and viscous model in the FTHE numerical study, it is apparent that the airflow encounters resistance, resulting in the formation of vortices around the tube. These vortices could potentially be considered reverse flow during simulation, but curiously, this phenomenon results in an increase in the thermal and hydraulic boundary layer around the tube, allowing for more even tube cooling. The airflow rate observed as it passes through the test section domain, as seen in Figure 9, shows that the FTHE with 358,456 grids and the standard viscous k-ω model averaged approximately 1.96 m/s at a flow velocity of 0.5 m/s and 7.76 m/s at a flow velocity of 3.5 m/s.

Figure 8 demonstrates the presence of flow separation in each geometry. The transverse geometry appears to have a more dominant wake region than the longitudinal geometry. The presence of a larger wake region results in less well-distributed heat transfer between the cold and hot fluids. The minimum velocity is shown in the geometry with a grid variation of 157653 with a minimum value of 1.4 m/s. This is indicated due to the variation of the viscous k-ω BSL (Baseline) model and allows for a higher swirl flow effect.

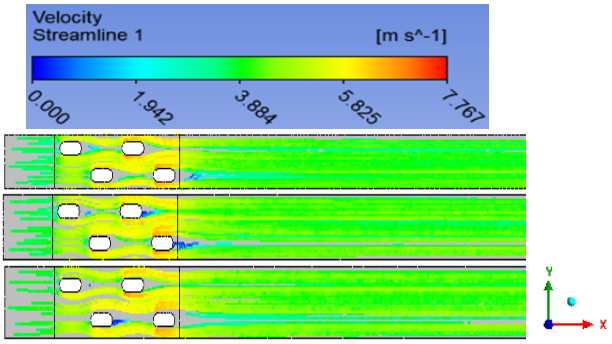

Figure 9. Velocity Streamline Contour of FTHE with Variations in the Number of Grids of 157653, 257892, and 358456 and a Flow Velocity Variation of 3.5 m/s

Figure 10 shows that stagnation and wake regions are visible, with the highest pressure contour appearing at the initial air-tube contact point, while the lowest contour is located behind the tube due to flow separation. This occurs precisely with a grid variation of 157,653 with a variation of the viscous k-ω BSL (Baseline) model, with the lowest pressure value of 69.45 Pa and the highest with 87.86 Pa. Furthermore, viscosity and drag at high speeds, friction between the air and the fin surface, cause a dominant pressure drop (high-pressure loss) in the FTHE with a grid number of 358,456 with a viscous k-ω Standard model with a lowest pressure value of 63.15 Pa and a highest value of 81.56 Pa. Thus, in the FTHE, increasing air velocity forces a more significant pressure drop, resulting in a pressure contour distribution with a high-pressure stagnation point at the front and a low-pressure wake region behind the tube.

However, when the velocity is not uniform across the FTHE surface, it will cause an uneven pressure contour distribution, potentially reducing heat transfer efficiency. The pressure contours in Figure 10 also visualize the fluid

pressure drop during flow, which is crucial for heat transfer efficiency. Numerical studies have shown that the highest pressure is often found at the inlet boundary conditions and drops dramatically at the outlet due to friction and velocity changes. These contours identify areas of high pressure drop in the FTHE geometry, which we will discuss in the next section.

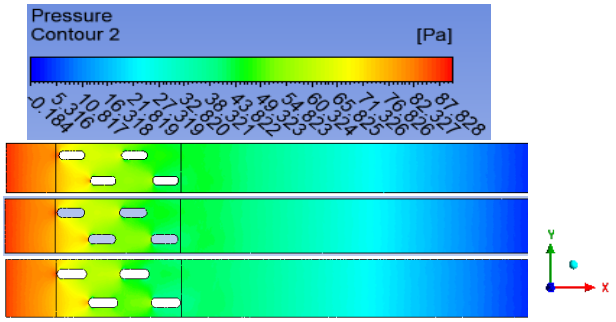

Figure 10. Velocity Streamline Contour of FTHE with Variations in the Number of Grids of 157653, 257892, and 358456 and a Flow Velocity Variation of 3.5 m/s.

Figure 11 presents a comparison between three turbulence models in simulating the relationship between Reynolds Number and Velocity. The graph shows a positive linear relationship for all three tested models. As the Reynolds Number increases from 1300 to 2500, velocity values also increase proportionally from around 1.5 m/s to nearly 8 m/s. The Standard k-ω model consistently produces the highest velocity estimates compared to the other two models at each Reynolds Number point, with a value of 7.76 m/s. The SST (Shear Stress Transport) k-ω model falls in the middle, showing a slightly lower velocity prediction than the Standard model, with a value of 7.48 m/s. The BSL (Baseline) k-ω model provides the lowest velocity prediction of the three, with a value of 7.2 m/s.

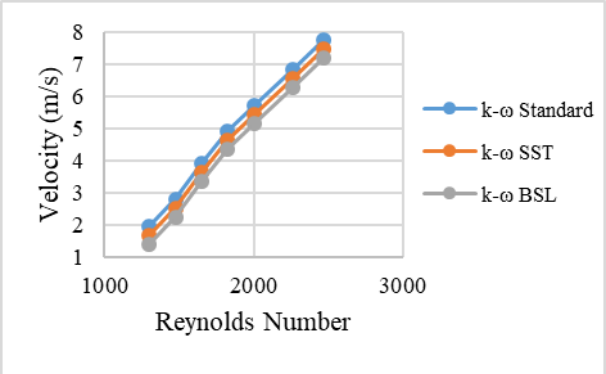

Figure 11. Graph of Velocity Values and Reynolds Numbers on Grid Variations 358456.

At Reynolds Numbers above 2000, turbulent flow characteristics (high velocities) increase fluid mixing, thereby increasing the rate of convective heat transfer (Nusselt number). The result is an increase in the heat transfer efficiency of the FTHE due to the increased heat transfer coefficient. However, increasing the speed can increase friction, which proportionally increases the heat transfer efficiency. Therefore, high speed (high Re) is desirable to maximize FTHE performance, despite increasing pressure drop.

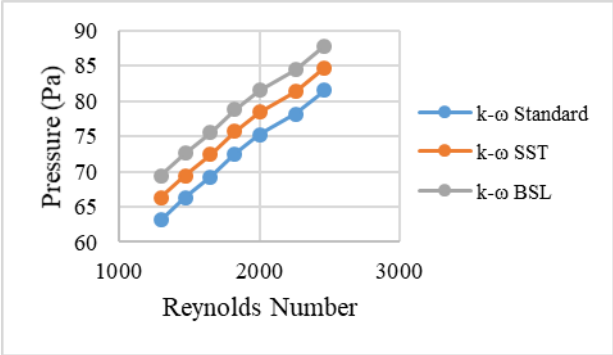

Figure 12. Graph of Pressure Values and Reynolds Numbers on Grid Variations 358456.

In Figure 12, it is explained that the graph shows a positive linear correlation between Reynolds Number and Pressure. As the Reynolds Number increases (from the range of 1300 to 2500), the resulting pressure also increases in the three simulation models. This is consistent with the principles of fluid mechanics, where increasing flow velocity (which usually causes a greater pressure drop or pressure loss due to friction and turbulence. Air pressure ranges from 63.15 Pa to 81.56 in the Standard k-ω model, which makes it the best result in this research.

Conclusions

Numerical studies on FTHE with the proposed variations in the number of grids and viscous models resulted in flow separation around the FTHE specimen, causing wakes and vortices around the tube, this phenomenon validates the differences in the number of grids and viscous models. The best results of this study were obtained at a variation of the number of grids of 358456 in the variation of the Standard viscous k-ω model with an average FTHE temperature value of 21.35ºC and a maximum heat transfer coefficient value of 101.74 W/m²K. The large

variation in the number of grids allows the computational network to be built with a high resolution so that it can capture the effects of thermal and hydraulic boundary layers accurately. The choice of the Standard viscous k-ω model in this research is because it has a suitability in numerical studies reviewed in terms of reductional costs during simulation and has accurate calculation results compared to other viscous models. These results confirm that the variation of the number of grids of 358456 in the variation of the Standard viscous k-ω model allows that the numerical study model can be recommended and used for practical applications in petrochemical processing, HVAC&R, and other machine devices because it is energy and cost efficient, as well as easy in production and maintenance aspects so that it can be applied directly in the field.

Thaks To
Beasiswa Pendidikan Indonesia (BPI). Gedung C Lantai 13.
Jl. Jenderal Sudirman Senayan, Jakarta Pusat 10270.

Efficiency and Conservation of Energy Laboratory, Department of Mechanical Engineering, Faculty of Engineering, Diponegoro University.
Jl. Prof. Sudarto No.13, Tembalang, Kec. Tembalang, Kota Semarang, Jawa Tengah (50275), Indonesia.

Energy Conversion Technology Laboratory, Department of Mechanical Engineering, Persatuan Guru Republik Indonesia Semarang University.
Jl. Pawitan Luhur III No.1, Bendan Duwur, Kec. Gajahmungkur, Kota Semarang, Jawa Tengah 50233.

References

[1]. M. Safi'i, N. Sinaga, M. Khoirunnisa, M. I. F. P. Arya, A. Nugroho, T. Priangkoso, Susanto, S. Suheri, O. Heriyani, Y. Effendi. "Studi Numerik Pengaruh Variasi Longitudinal dan Transversal Pitch terhadap Performa Fin and Tube Heat Exchanger". *Momentum*, 20 (*2*), 159-168, 2025. http://dx.doi.org/10.36499/jim.v20i1.11945.

[2]. A. Nugroho, M. Safi'i, B. P. Romadhon, M. A. Wahid, M. E. Pujianto. "Numerical Study on the Effect of Box and Polygon Geometry In Fin and Tube Heat Exchanger on Fluid Flow and Heat Transfer". *Jurnal Polimesin*. 22 (*6*), 638-645, 2024. http://dx.doi.org/10.30811/jpl.v22i6.5624.

[3]. A. A. Bhuiyan, A. K. M. S. Islam., (2016). "Thermal and Hydraulic Performance of Finned-Tube Heat Exchangers Under Different Flow Ranges: A Review on Modeling and Experiment". *International Journal of Heat and Mass Transfer*, 101 (*10*), 38-59, 2016. http://dx.doi.org/10.1016/j.ijheatmasstransfer.2016.05.022.

[4]. A. A. Bhuiyan, M. R. Amin, A. K. M. S. Islam, (2013). "Three-Dimensional Performance Analysis of Plain Fin Tube Heat Exchangers in Transitional Regime", *Applied Thermal Engineering*. 50 (*1*), 445-454. 2013. http://dx.doi.org/10.1016/j.applthermaleng.2012.07.034.

[5]. Y. Wang, Z. Su, Z. Huang, L. Shi, H. Dong. "Numerical Study on the Efficiency Improvement of Household Thermal Energy Storage Device by Optimized Finned Tube Heat Exchanger". *Applied Thermal Engineering*. 275 (*9*), 1-14, 2025. https://doi.org/10.1016/j.applthermaleng.2025.126816.

[6]. J. Batista, Anica Trp, K. Lenic, M. Kirincic. "The Influence of Geometry Parameters of Rectangular Vortex Generators on the Air-to-Water Fin-and-Tube Heat Exchanger Efficiency Enhancement. *International Communications in Heat and Mass Transfer*. 162 (*3*), 1-13, 2025. https://doi.org/10.1016/j.icheatmasstransfer.2025.108647.

[7]. W. Hu, W. Ye, Y. Guan, X. Zhang, C. Jiang, Z. Li. "Enhancing the Thermal Hydraulic Performance on the Air Side of Finned Tube Heat Exchangers Through Superhydrophilic–Superhydrophobic Striped Patterns". *Thermal Science and Engineering Progress*. 70 (*2*), 1-14, 2026. https://doi.org/10.1016/j.tsep.2026.104503.

[8]. B. K. Choure, T. Alam, R. Kumar. Melting and Solidification Performance of Dimple Shape, Multitube and Fins Applied PCM Based Triple Tube Heat Exchanger". *Journal of Energy Storage*. 152 (*2*), 1-15, 2026. https://doi.org/10.1016/j.est.2026.120650.

[9]. B. Masoumpour, M. Ataeizadeh, H. Hajabdollahi, M. S. Dehaj. "Performance Evaluation of a Shell and Tube Heat Exchanger with Recovery of Mass Flow Rate". *Journal of the Taiwan Institute of Chemical Engineers*. 000. (*1*), 1-13, 2021. https://doi.org/10.1016/j.jtice.2021.05.022.

[10]. J. Zhou, X. Xie, S. Tang, Y. Xu, X. Li. "Numerical Investigation and Comparison on Thermal-hydraulic Performance of H-type Finned Tube Heat Exchanger". *Case Studies in Thermal Engineering*. 59. (*1*), 1-13, 2024. https://doi.org/10.1016/j.csite.2024.104481.

[11]. M. S. S. Efanden, F. E. Sapnken, A. K. Jeutsa, B. S. S. Diboma, J. G. Tamba. "Performance Analysis of Air-to-Ground Heat Exchanger in Equatorial Yaoundé: Hourly and Daily Thermal Behaviour and Efficiency Optimization". *Journal of Building Engineering*. 96 (*1*) 1-12, 2024. https://doi.org/10.1016/j.jobe.2024.110396.

[12]. R. Saltarelli, L. M. Alves, M. Fasano, R. M. Afonso. "Joining by Forming Technology for Thermal Applications: A Case Study of Finned Tube Heat Exchanger". *Case Studies in Thermal Engineering*. 59, (*1*), 1-10, 2024. https://doi.org/10.1016/j.csite.2024.104551.

[13]. V. Safari, B. Kamkari, A. Gharbi. "Wedge-shaped Fins to Enhance Thermal Performance of Shell and Tube Heat Exchangers Containing Phase Change Material: An Experimental Study". *Thermal Science and Engineering Progress*. 49 (*1*), 1-10, 2024. https://doi.org/10.1016/j.tsep.2024.102474.

[14]. Z. Bai, A. M. Abed, P. K. Singh, D. Abduvalieva, S. Alkhalaf, Y. Elmasry, A. Alruwaili, F. S. Alharbi, F. Riaz. "Bow-shaped Vortex Generators in Finned-tube Heat Exchangers; ANN/GA-Based Hydrothermal/Structural Optimization". *Case Studies in Thermal Engineering*. 55 (*1*), 1-20, 2024. https://doi.org/10.1016/j.csite.2024.104135.

[15]. M. Reshaeel, M. Abdelsamie, M. I. H. Ali. "A Critical Review of the Thermal-Hydraulic Performance of Fin and Tube Heat Exchangers using Statistical Analysis". *International Journal of Thermofuids*. 24 (*1*), 1-35, 2024. https://doi.org/10.1016/j.ijft.2024.100858.

[16]. T. Zhang, M. Su, H. Zhang, C. Liu, X. Ouyang. "Design and Simulation of a New Type of Fin-and-tube Heat Exchanger with Trapezoidal Slit Fins". Case Studies in Thermal Engineering. 59 (*1*), 1-12, 2024. https://doi.org/10.1016/j.csite.2024.104604.

[17]. X. Y. Zhang, Y. T. Ge, Y. Burra, P.Y. Lang. "Experimental Investigation and CFD Modelling Analysis of Finned-tube PCM Heat Exchanger for Space Heating". *Applied Thermal Engineering*. 244 (*1*), 1-18, 2024. https://doi.org/10.1016/j.applthermaleng.2024.122731.

[18]. M. Boujelbene, H. I. Mohammed, H. S. Sultan, M. Eisapour, Z. Chen, J. M. Mahdi, A. Cairns, P. Talebizadehsardari. "A Comparative Study of Twisted and Straight Fins in Enhancing the Melting and Solidifying Rates of PCM In Horizontal Double-Tube Heat Exchangers. *International Communications in Heat and Mass Transfer*. 151 (*1*), 1-12, 2024. https://doi.org/10.1016/j.icheatmasstransfer.2023.107224.

[19]. J. Zhou, Z. Shi, S. Tang, K. Zhao. "Dynamic Modeling of Heat and Mass Transfer in Photovoltaic-Electrolyzer Systems: Implications for System Design and Safety". *Applied Energy*. 403 (1), 1-15, 2026. https://doi.org/10.1016/j.apenergy.2025.127029.

[20]. A. Aldaghi, M. Mohammadi, A. Taheri, M. Passandideh-Fard. "On The Performance of a Latent Heat Thermal Storage Unit Integrated with a Helically Coiled Copper Tube and Organic Phase Change Materials: a Lab-Scale Experimental Study". *International Communications in Heat and Mass Transfer***.** 154 (5), 1-12, 2024. https://doi.org/10.1016/j.icheatmasstransfer.2024.107403.

[21]. A. Alizadeh, K. Kriaa, A. M. Mohsen, M. Mazen, Othayq, M. M. Al-Zahiwat, A. M. Sadeq, H. Rajab, K. Hajlaoui. "Numerical and statistical Analysis of Hybrid Nanofluid Impact on Finned Shell and coil Heat Exchanger Performance". Journal of Engineering Research. 10 (1), 1-20, 2026. https://doi.org/10.1016/j.jer.2026.02.005.

[22]. A. Vahabi, S. Abdolmehdi Hashemi, A. Fattahi. "Performance Optimization of a Finned-Curved Tubes Compact Heat Exchanger: Numerical Simulation and Machine Learning Method". Case Study In Thermal Engineering. 73 (1), 1-19, 2026. https://doi.org/10.1016/j.csite.2025.106477.